Rock Mech. Rock Engng. (2000) 33 (2), 75–92

Rock Mechanics and Rock Engineering

Strain-dependent Fluid Flow Defined Through Rock Mass Classification Schemes

By

J. Liu[1,2], **D. Elsworth**[3], **B. H. Brady**[4], and **H. B. Muhlhaus**[1]

[1] CSIRO Exploration and Mining, Nedlands, Australia
[2] Center for Oil and Gas Engineering, The University of Western Australia, Nedlands, Australia
[3] Department of Energy and Geo-Environmental Engineering, The Pennsylvania State University, University Park, PA, U.S.A.
[4] Faculty of Engineering and Mathematical Science, University of Western Australia, Nedlands, Australia

Summary

Strain-dependent hydraulic conductivities are uniquely defined by an environmental factor, representing applied normal and shear strains, combined with intrinsic material parameters representing mass and component deformation moduli, initial conductivities, and mass structure. The components representing mass moduli and structure are defined in terms of RQD (rock quality designation) and RMR (rock mass rating) to represent the response of a whole spectrum of rock masses, varying from highly fractured (crushed) rock to intact rock. These two empirical parameters determine the hydraulic response of a fractured medium to the induced-deformations. The constitutive relations are verified against available published data and applied to study one-dimensional, strain-dependent fluid flow. Analytical results indicate that both normal and shear strains exert a significant influence on the processes of fluid flow and that the magnitude of this influence is regulated by the values of RQD and RMR.

1. Introduction

A knowledge of changes in hydraulic conductivity that result from the redistribution of stresses or strains around engineered structures is crucially important. Changes in hydraulic conductivity, as a result of thermoporomechanical coupling in a radioactive waste repository, may impact the spread of aqueous and colloidal contaminants (Pusch, 1989; Smelser et al., 1984; Skoczylas and Henry, 1995). Changes in hydraulic conductivity due to underground excavation may affect groundwater inflows into tunnels, create difficult tunnelling conditions and slow the advance rate (Zhang and Franklin, 1993; Wei et al., 1995; Jakubick and Franz, 1993). Changes in hydraulic conductivity due to the redistribution of stresses within coal seams affect the diffusion and flow of methane, thus influenc-

ing the rate of emission of coal-bed methane into both underground mine workings and to the environment as a greenhouse gas (Smelser et al., 1984; Patton et al., 1994; Valliappan and Zhang, 1996). Underground mining potentially induces large strains in the overlying strata, that in turn may result in the development of a strongly heterogeneous and anisotropic hydraulic conductivity field. This strain-dependent conductivity field is of special importance in evaluating the potential impact of underground mining on ground water resources (Neate and Whittaker, 1979; Booth, 1992; Walker, 1988; Roosendaal et al., 1990). The local ground water system may be appreciably altered (Matetic et al., 1991; Matetic and Trevits, 1992; Matetic, 1993; Matetic et al., 1995). It is apparent that stress-dependent flow laws are of central importance to a wide range of engineering problems.

The hydraulic conductivity of a fracture is primarily determined by the aperture of the fracture. The aperture is affected by both the normal and shear deformation. Laboratory studies (Jones, 1975; Nelson and Handin, 1977; Kranz, 1979; Trimmer et al., 1980) have documented this observation, and theoretical models (Bawden et al., 1980; Ayatollahi et al., 1983) are capable of replicating this behavior. To a residual threshold, there is decrease in fracture conductivity with increasing normal load. Shear displacements influence conductivity, as conditioned by fracture aperture and roughness (Brown, 1987), and there is evidence that dilatancy plays a central role, especially under low ambient stresses (Teufel, 1987; Makurat, 1985; Makurat et al., 1990). At higher stresses, crushing of asperities, and the production of gouge may reduce stresses. Thus, the ambient stress field governs the fluid transmission behavior of fractures and can explain why fractures may, at different times, be both a conductor and a barrier to fluid flow (Hooper, 1990). Results reporting stress-dependent conductivity for the complete stress-strain curve (Li et al., 1994) and for true triaxial conditions (King et al., 1995) have also been reported. These experimental results provide critical physical insights into complex hydro-mechanical processes. Alvarez et al. (1995) concluded, by re-evaluating published experiments, that relations between hydraulic aperture and fracture closure are generally linear at low effective normal stresses ($<$25 MPa) and in some studies depart from a straight line as an irreducible flow rate is approached at higher stresses. Assuming the *cubic law* is valid for fracture flow, Ouyang and Elsworth (1993) define the relationship between induced-normal strain and hydraulic conductivity for two-dimensional cases. Based on this theoretical relationship, a three-dimensional relationship between induced-normal strain and hydraulic conductivity has been developed by Liu (1996), and applied in the study of longwall mining (Matetic et al., 1995; Liu, 1994; Liu and Elsworth, 1997; Liu et al., 1997). In these studies, the existing normal strain-permeability relations (Liu, 1996) are modified and extended to include the dilatancy effects due to shear strains. More importantly, the new strain-permeability constitutive relations are defined by two valuable empirical parameters, RQD (rock quality designation) (Sen, 1997) and RMR (rock mass rating) (Nicholson and Bieniawski, 1990), both of which are readily available in practice. Based on these stress-permeability constitutive relations, a stress-dependent relation is developed in the following for one-dimensional flow, and verified against available published data.

2. Approach

A general form of the governing equation for fluid flow in fractured media is defined as

$$\frac{\partial}{\partial x_j}\left(K_{ij}\frac{\partial h}{\partial x_i}\right) = S_s\frac{\partial h}{\partial t}, \tag{1}$$

where K_{ij} are components of the hydraulic conductivity tensor, h is total hydraulic head, x_i $(i = 1, 2, 3)$ is coordinates, S_s is specific storage, and t is time. The flow velocity, V_i, is defined as

$$V_i = -K_{ij}\frac{\partial h}{\partial x_i}. \tag{2}$$

In this study, the hydraulic conductivity, K_{ij}, is defined as a function of changes in strain.

The following assumptions are made for the derivation of the strain-conductivity relations.

1. The rock mass can be represented as two-dimensional or three-dimensional orthogonally fractured media. Under this assumption, fracture apertures may be defined as a joint function of the initial hydraulic conductivity and fracture spacings;
2. No new fractures are produced during deformation and fracture spacings correspondingly remain unchanged. Under this assumption, the strain-dependent hydraulic conductivity field can be defined as a function of the initial conductivity and the induced-strain field;
3. The rock matrix is functionally impermeable and the dominant fluid flow is within the fractures. Correspondingly, changes in conductivity can be defined by the equivalent parallel plate model (Witherspoon et al., 1980);
4. Extensional strains increase the directional hydraulic conductivity, and compressive strains decrease conductivity.

Reductions in compression are typically truncated by a residual threshold. Accordingly, these assumptions limit the range of applicability of these strain-conductivity relations. For example, it may not be appropriate to apply these relations for shearing under high normal stress-to-strength ratios where gouge formation and fracture plugging, or fracture contraction, may be important processes (Makurat and Gutierrez, 1996).

3. Strain-dependent Hydraulic Conductivity

The revised hydraulic conductivity fields can be determined if changes in fracture aperture can be defined as a function of induced-strains. This is realized by partitioning the induced-strains between fracture and solid matrix. These results are reported in the following.

3.1 Two-dimensional Case

Assuming deformations in normal closure or extension are the predominant conductivity-enhancing mode, the directional hydraulic conductivities, K_x and K_y, in the x- and y-directions, are defined by Ouyang and Elsworth (1993) as

$$\begin{cases} K_x = \dfrac{\mathrm{g}}{12\mu s}(b + \Delta b_y)^3 \\ K_y = \dfrac{\mathrm{g}}{12\mu s}(b + \Delta b_x)^3, \end{cases} \tag{3}$$

where g is gravitational acceleration, μ is kinematic viscosity, s is the fracture spacing, and Δb_x and Δb_y are, respectively, displacements in the x- and y-directions, on fractures that are orthogonal to the displacement, as illustrated in Fig. 1.

In the following, Eq. 3 is modified to include the effect of shear stresses on the hydraulic conductivity. As illustrated in Fig. 1, changes in fracture aperture, Δb_x and Δb_y, may result from both normal deformation and shear deformation, as defined as

$$\begin{cases} \Delta b_x = \Delta b_{xn} + \Delta b_{xs} \\ \Delta b_y = \Delta b_{yn} + \Delta b_{ys}, \end{cases} \tag{4}$$

where Δb_{xn} and Δb_{xs} are the induced-displacements in the x-direction on the fractures due to the induced-normal strain, $\Delta\varepsilon_x$, and the induced-shear strain, $\Delta\gamma_{xy}$, respectively; Δb_{yn} and Δb_{ys} are the induced-displacements in the y-direction on the fractures due to the induced-normal strain, $\Delta\varepsilon_y$, and the induced-shear strain, $\Delta\gamma_{xy}$, respectively. It is clear that $\Delta b_{xs} = \Delta b_{ys}$ since $\Delta\tau_{xy} = \Delta\tau_{yx}$. As illustrated in Figs. 1(b) and (c), the displacements onto the vertical fracture and the horizontal fracture due to the induced-normal strains in the x- and y-directions, Δb_{xn} and Δb_{yn}, are defined as

$$\begin{cases} \Delta b_{xn} = \dfrac{1}{E}(\Delta\sigma_x - \nu\Delta\sigma_y)(s+b) - \dfrac{1}{E_r}(\Delta\sigma_x - \nu\Delta\sigma_y)s = (\Delta\sigma_x - \nu\Delta\sigma_y)\left[\dfrac{s+b}{E} - \dfrac{s}{E_r}\right] \\ \Delta b_{yn} = \dfrac{1}{E}(\Delta\sigma_y - \nu\Delta\sigma_x)(s+b) - \dfrac{1}{E_r}(\Delta\sigma_y - \nu\Delta\sigma_x)s = (\Delta\sigma_y - \nu\Delta\sigma_x)\left[\dfrac{s+b}{E} - \dfrac{s}{E_r}\right], \end{cases} \tag{5}$$

where $\Delta\sigma_x$, $\Delta\sigma_y$ and $\Delta\tau_{xy}$ are normal and shear stress components, respectively; $\Delta\varepsilon_x$, $\Delta\varepsilon_y$ and $\Delta\gamma_{xy}$ are induced normal and shear strain components, respectively; E and ν are elastic modulus and Poisson ratio of the rock mass, and E_r is the elastic modulus of the intact rock. Substituting $E = R_e E_r$ into Eq. 5 gives

$$\begin{cases} \Delta b_{xn} = [b + s(1 - R_e)]\Delta\varepsilon_x \\ \Delta b_{yn} = [b + s(1 - R_e)]\Delta\varepsilon_y, \end{cases} \tag{6}$$

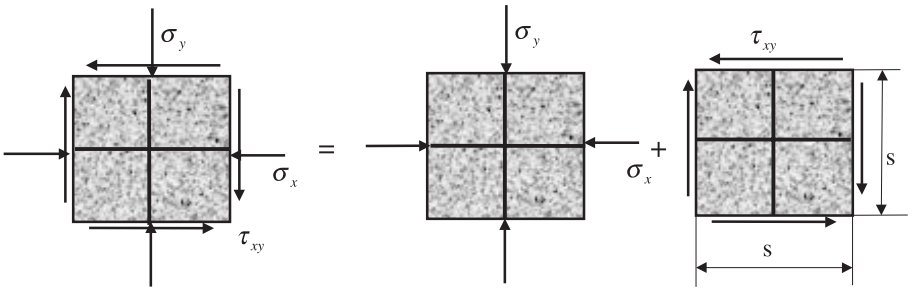

(a) Principle of Superposition

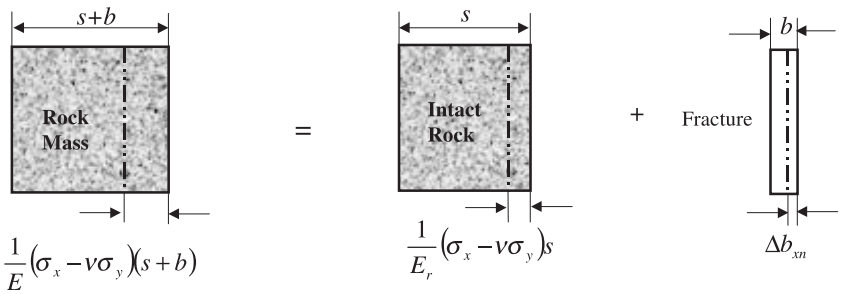

(b) Relation among Components of the Displacement in the x-Direction due to Normal Stress

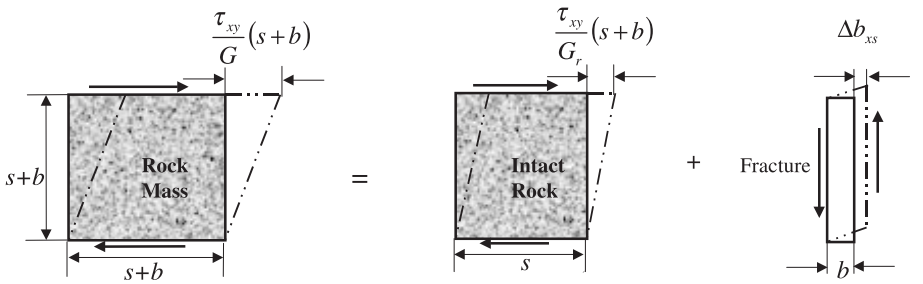

(c) Relation among Components of the Displacement in the x-Direction due to Shearing

Fig. 1. A schematic representation of an isolated rock mass body. Identical fractures are present with spacing, *s*, and aperture, *b*

where R_e is defined as the ratio of the elastic modulus of rock mass to that of the rock matrix.

Through the same procedure as above, the displacements applied to the vertical and horizontal fractures due to the induced-shear strains in the x- and y-directions, Δb_{xs} and Δb_{ys}, are defined as

$$\begin{cases} \Delta b_{xs} = \dfrac{1}{G}\Delta\tau_{xy}(s+b) - \dfrac{1}{G_r}\Delta\tau_{xy}s = (s+b)(1-R_g)\Delta\gamma_{xy} \\ \Delta b_{ys} = \dfrac{1}{G}\Delta\tau_{yx}(s+b) - \dfrac{1}{G_r}\Delta\tau_{yx}s = (s+b)(1-R_g)\Delta\gamma_{yx}, \end{cases} \tag{7}$$

where G_r and G are the shear modulus for intact rock and rock mass, respectively. $R_g = G/G_r$ is defined as the shear modulus reduction ratio.

Assuming that the normal stress-to-strength ratios are low, shear strains always increase hydraulic conductivity (Makurat and Gutierrez, 1996). Therefore, the shear strains in Eq. 7 should be replaced by their absolute values. Constitutive relations between induced-strains and fracture apertures are obtained by substituting Eqs. 5 through 7 into Eq. 4 as

$$\begin{cases} \Delta b_x = [b + s(1 - R_e)]\Delta\varepsilon_x + (s + b)(1 - R_g)|\Delta\gamma_{xy}| \\ \Delta b_y = [b + s(1 - R_e)]\Delta\varepsilon_y + (s + b)(1 - R_g)|\Delta\gamma_{xy}|. \end{cases} \tag{8}$$

Subsequently, strain-dependent hydraulic conductivities are obtained by substituting Eqs. 8 into 3 as

$$\begin{cases} K_x = \dfrac{\mathrm{g}}{12\mu s}\{b + [b + s(1 - R_e)]\Delta\varepsilon_y + (s + b)(1 - R_g)|\Delta\gamma_{xy}|\}^3 \\ K_y = \dfrac{\mathrm{g}}{12\mu s}\{b + [b + s(1 - R_e)]\Delta\varepsilon_x + (s + b)(1 - R_g)|\Delta\gamma_{xy}|\}^3. \end{cases} \tag{9}$$

Substituting $K_0 = \dfrac{gb^3}{12\mu s}$ into Eq. 9 yields

$$\begin{cases} \dfrac{K_x}{K_0} = \left\{1 + \left[1 + \dfrac{2(1 - R_e)}{\phi_f}\right]\Delta\varepsilon_y + \left(1 + \dfrac{2}{\phi_f}\right)(1 - R_g)|\Delta\gamma_{xy}|\right\}^3 \\ \dfrac{K_y}{K_0} = \left\{1 + \left[1 + \dfrac{2(1 - R_e)}{\phi_f}\right]\Delta\varepsilon_x + \left(1 + \dfrac{2}{\phi_f}\right)(1 - R_g)|\Delta\gamma_{xy}|\right\}^3, \end{cases} \tag{10}$$

where ϕ_f is the effective porosity and is defined as

$$\phi_f = \frac{(b + s)^2 - s^2}{(b + s)^2} \cong \frac{2b}{s}. \tag{11}$$

For simplicity, Eq. 10 is symbolically written as

$$\frac{K_{ii}}{K_0} = \left\{1 + \left[1 + \frac{2(1 - R_e)}{\phi_f}\right]\Delta\varepsilon_{jj} + \left(1 + \frac{2}{\phi_f}\right)(1 - R_g)|\Delta\gamma_{ij}|\right\}^3, \tag{12}$$

where K_{ii} $(i = x, y)$ represents directional conductivities, and $\Delta\varepsilon_{jj}$ $(j = x, y)$ and $\Delta\gamma_{ij}$ $(i, j = x, y)$ represent induced-strains. As shown in Eq. 10, the strain dependent hydraulic conductivities are uniquely defined by parameters, R_e, R_g and ϕ_f for the original rock mass, and by the induced-strains.

3.2 Three-dimensional Case

For three-dimensional orthogonally fractured media, changes in one-directional hydraulic conductivity are a function of induced-strains in the other two orthogo-

nal directions. Therefore, Eqs. 12 and 11 can be easily extended to the 3-D case as:

$$\frac{K_{ii}}{K_0} = \frac{1}{2}\left\{1 + \left[1 + \frac{3(1-R_e)}{\phi_f}\right]\Delta\varepsilon_{jj} + \left(1 + \frac{3}{\phi_f}\right)(1-R_g)|\Delta\gamma_{jk}|\right\}^3 + \frac{1}{2}\left\{1 + \left[1 + \frac{3(1-R_e)}{\phi_f}\right]\Delta\varepsilon_{kk} + \left(1 + \frac{3}{\phi_f}\right)(1-R_g)|\Delta\gamma_{kj}|\right\}^3, \quad (13)$$

$$\phi_f = \frac{(b+s)^3 - s^3}{(b+s)^3} \cong \frac{3b}{s} \quad (14)$$

respectively. For practical purposes, the constitutive relations between strains and directional hydraulic conductivities in fractured porous media, as defined by Eq. 12 for the 2-D case, and by Eq. 13 for the 3-D case, are simplified as

$$\frac{K_{ii}}{K_0} = \left[1 + \frac{2(1-R_e)}{\phi_f}\Delta\varepsilon_{jj} + \frac{2(1-R_g)}{\phi_f}|\Delta\gamma_{ij}|\right]^3 \quad (15)$$

and

$$\frac{K_{ii}}{K_0} = \frac{1}{2}\left[1 + \frac{3(1-R_e)}{\phi_f}\Delta\varepsilon_{jj} + \frac{3(1-R_g)}{\phi_f}|\Delta\gamma_{jk}|\right]^3 + \frac{1}{2}\left[1 + \frac{3(1-R_e)}{\phi_f}\Delta\varepsilon_{kk} + \frac{3(1-R_g)}{\phi_f}|\Delta\gamma_{kj}|\right]^3 \quad (16)$$

respectively. Assuming $R_e = R_g = 1$, Eq. 12 for the 2-D case, and Eq. 13 for the 3-D case, can be simplified to represent the constitutive relations connecting induced-strains with hydraulic conductivities in porous media as

$$\frac{K_{ii}}{K_0} = (1 + \Delta\varepsilon_{jj})^3 \quad (17)$$

and

$$\frac{K_{ii}}{K_0} = \frac{1}{2}(1 + \Delta\varepsilon_{jj})^3 + \frac{1}{2}(1 + \Delta\varepsilon_{kk})^3 \quad (18)$$

respectively.

3.3 Definitions of R_e and R_g

As illustrated in Fig. 1(c), shear and dilation are related through the equivalent and intact moduli, as

$$\frac{\tau_{xy}}{G}(s+b) = \frac{\tau_{xy}}{G_r}s + \frac{\tau_{xy}}{K_s}\tan\phi_d, \quad (19)$$

where K_s is the fracture shear stiffness, and ϕ_d is the fracture dilatational angle. Equation 19 may be rearranged to yield

$$R_g = \frac{1 + \dfrac{b}{s}}{1 + \dfrac{G_r}{sK_s}\tan\phi_d} = \frac{1 + 0.5\phi_f}{1 + \dfrac{G_r}{sK_s}\tan\phi_d}. \tag{20}$$

As shown in Eq. 20, the resulting shear modulus reduction ratio is a function of the effective porosity, ϕ_f, and the mass compliance, $\dfrac{G_r}{sK_s}\tan\phi_d$. Theoretically, R_g varies between zero $\left(\dfrac{G_r}{sK_s}\tan\phi_d \to \infty\right)$ and unity $\left(\dfrac{G_r}{sK_s}\tan\phi_d \to 0.5\phi_f\right)$. Similarly, R_e is defined as

$$R_e = \frac{E}{E_r} = \frac{1 + 0.5\phi_f}{1 + \dfrac{E_r}{sK_n}}, \tag{21}$$

where K_n is the fracture normal stiffness. As shown in Eq. 21, the resulting modulus reduction ratio is a function of the effective porosity, ϕ_f, and the mass compliance, E_r/sK_n. Theoretically, R_e varies between zero $(E_r/sK_n \to \infty)$ and unity $(E_r/sK_n \to 0.5\phi_f)$.

3.4 Determination of R_e and R_g

R_e and R_g may be correlated with rock mass classification schemes. R_e and R_g are actually a measure of scale effect, defined as the variation of any functional parameter, perhaps strength, modulus or permeability, with specimen size. For application to field problems, laboratory values of deformation moduli should be reduced (Nicholson and Bieniawski, 1990; Mohammad et al., 1997). According to a variety of results (Nicholson and Bieniawski 1990), R_e and R_g may be defined as a function of RMR

$$R_e = R_g = 0.000028\mathrm{RMR}^2 + 0.009e^{\mathrm{RMR}/22.82}, \tag{22}$$

where RMR is defined as rock mass rating (Bieniawski, 1978). This rock mass classification utilizes the following six parameters, all of which are measurable in the field and can also be obtained from borehole data:

1. uniaxial compressive strength of the intact rock material;
2. rock quality designation (RQD);
3. spacing of the discontinuities;
4. condition of the discontinuities;
5. groundwater conditions;
6. orientation of the discontinuities.

The classification scheme quantifies rock mass conditions according to a scale varying from 0 to 100. Highly fractured (crushed) rock approaches an RMR value of zero, while intact rock approaches 100.

3.5 Determination of ϕ_f

Substituting $b = \left(\frac{12\mu s K_0}{g}\right)^{1/3}$ into Eqs. 11 and 14 gives the effective porosity for the 2-D and and 3-D cases as

$$\phi_f = 2\left(\frac{12\mu K_0}{g s^2}\right)^{1/3} \tag{23}$$

and

$$\phi_f = 3\left(\frac{6\mu K_0}{g s^2}\right)^{1/3} \tag{24}$$

respectively. The equivalent fracture spacing, s, may be determined by an empirical rock classification index, RQD (Rock Quality Designation), which is defined as (Sen, 1997)

$$\mathrm{RQD} = 100 \sum_{i=1}^{n} \frac{X_i}{L}, \tag{25}$$

where n is the number of intact lengths greater than 10 cm, L is the length of a drill hole or scanline, and X_i is the intact length. Based on the value of RQD, rock masses are classified as five categories, namely: excellent ($90 < \mathrm{RQD} < 100$); very good ($75 < \mathrm{RQD} < 90$); fair ($50 < \mathrm{RQD} < 75$); poor ($25 < \mathrm{RQD} < 50$); and very poor ($0 < \mathrm{RQD} < 25$). Assuming that fractures occur randomly in nature and that the number of fractures along a borehole follow the Poisson process, so that the intact lengths have a negative exponential distribution, Priest and Hudson (1976) derived the following relation

$$\mathrm{RQD} = 100(1 + 0.1\lambda)e^{-0.1\lambda}, \tag{26}$$

where λ is the average number of fractures per meter. Substituting $s = 1/\lambda$ into Eq. 26 gives

$$\mathrm{RQD} = 100\left(1 + \frac{1}{10s}\right)e^{-(1/10s)}, \tag{27}$$

where s is the equivalent fracture spacing. The incorporation of RQD into the determination of effective porosity makes it possible to link the effective porosity to an empirical geotechnical parameter which is readily measured, in practice. When RQD approaches zero, it suggests that the rock mass approaches the form of a porous medium with a high effective porosity. When $\mathrm{RQD} = 100$, it suggests that the rock mass is relatively impermeable.

4. Sensitivity Study

As shown in Eqs. 15 and 16, the strain-dependent hydraulic conductivity, K_{ii} ($i = x, y, z$), is uniquely defined by the environmental factors (strains) and mate-

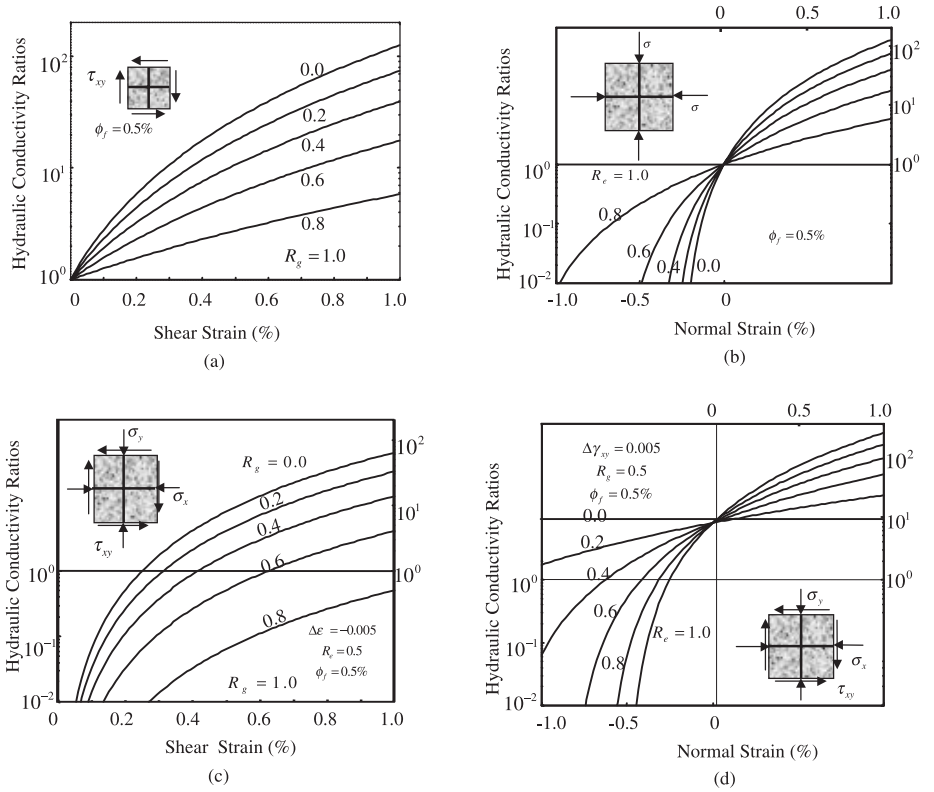

Fig. 2. Relations between induced-shear strains, $\Delta\gamma_{xy}$, normal strains, $\Delta\varepsilon_x$ and $\Delta\varepsilon_y$, and hydraulic conductivity ratios, K_{xx}/K_0 or K_{yy}/K_0: **a** pure shearing; **b** pure compression and extension; **c** complex stress state with constant normal strains; **d** complex stress state with constant shear strains

rial properties (R_e, R_g and ϕ_f). The effects of these intrinsic factors on changes in hydraulic conductivity are demonstrated in Fig. 2. Assuming $\Delta\varepsilon_{ii} = 0$, $\phi_f = 0.5\%$, Eq. 15 is reproduced graphically in Fig. 2(a). The hydraulic conductivity may increase by up to 2 orders of magnitude when R_g varies from 0 to 1. When the shear modulus reduction ratio, R_g, is equal to 1, the rock mass and the rock matrix material shear moduli are identical, and the shear strain is uniformly distributed between fracture and matrix. This results in the smallest possible change in hydraulic conductivity. When $R_g = 0$, the shear strain is applied entirely to the fracture system and precipitates the largest possible change in hydraulic conductivity. For the pure shearing case, changes in hydraulic conductivity are regulated by the shear modulus reduction ratio, R_g. Assuming $\Delta\gamma_{ij} = 0$, $\phi_f = 0.5\%$, Eq. 15 is graphically illustrated in Fig. 2(b). The hydraulic conductivity may increase by up to 2 orders of magnitude when the normal strain is positive and R_e varies from 0 to 1. The hydraulic conductivity may also decrease by up to 2 orders of magnitude when the normal strain is negative and R_e varies from 0 to 1. When the elastic modulus reduction ratio, R_e, is equal to 1, the rock mass and the rock matrix

material elastic moduli are identical, and the normal strain is uniformly distributed between fracture and matrix. This results in the smallest possible change in hydraulic conductivity. When $R_e = 0$, the normal strain is applied entirely to the fracture system and precipitates the largest possible change in hydraulic conductivity. For the pure compressive or extensional cases, changes in hydraulic conductivity are regulated by the elastic modulus reduction ratio, R_e. As shown in Figs. 2(c) and (d), both normal and shear strains may exert significant influence on strain-induced changes in hydraulic conductivity. The magnitudes of hydraulic conductivity ratios are regulated by R_e, R_g and ϕ_f.

5. Verification

The performance of the proposed strain-conductivity relations in this study has been compared with both the Gangi (Gangi, 1978) and Barton-Bandis (Barton et al., 1985) models. These results are reported in the following.

5.1 Comparison with the Gangi Model

Equation 17 is verified against Gangi's model. Gangi defined the relation between hydraulic conductivity and stress as

$$\frac{K}{K_0} = \left[1 - \frac{1}{2}\left(\frac{\Delta\sigma_c + \Delta\sigma_i}{E_0}\right)^{2/3}\right]^4, \tag{28}$$

where $\Delta\sigma_i$ is the equivalent cementing pressure; E_0 is the effective modulus of the grains, and $\Delta\sigma_c$ is the confining stress. Assuming the strain can be expressed as

$$\Delta\varepsilon = \frac{\Delta\sigma}{E} = \frac{\Delta\sigma_c + \Delta\sigma_i}{E_0}, \tag{29}$$

then Eq. 28 may be reformulated as

$$\frac{K}{K_0} = \left[1 - \frac{1}{2}(\Delta\varepsilon)^{2/3}\right]^4, \tag{30}$$

while the proposed relation is defined by Eq. 17. The relation proposed in this work (Eq. 17) is compared with the Gangi model (Eq. 30) and is shown in Fig. 3(a), in response to the variation of hydraulic conductivity ratio, K/K_0, versus strain, $\Delta\varepsilon$. The models exhibit favorable agreement, particularly when $\Delta\varepsilon = -1.0$, the proposed equation yields a more reasonable value ($K/K_0 = 0$).

5.2 Comparison with the Barton-Bandis Model

In the Barton-Bandis model (Barton et al., 1985), a distinction between mechanical and hydraulic apertures has been made. Based on the equivalent smooth wall

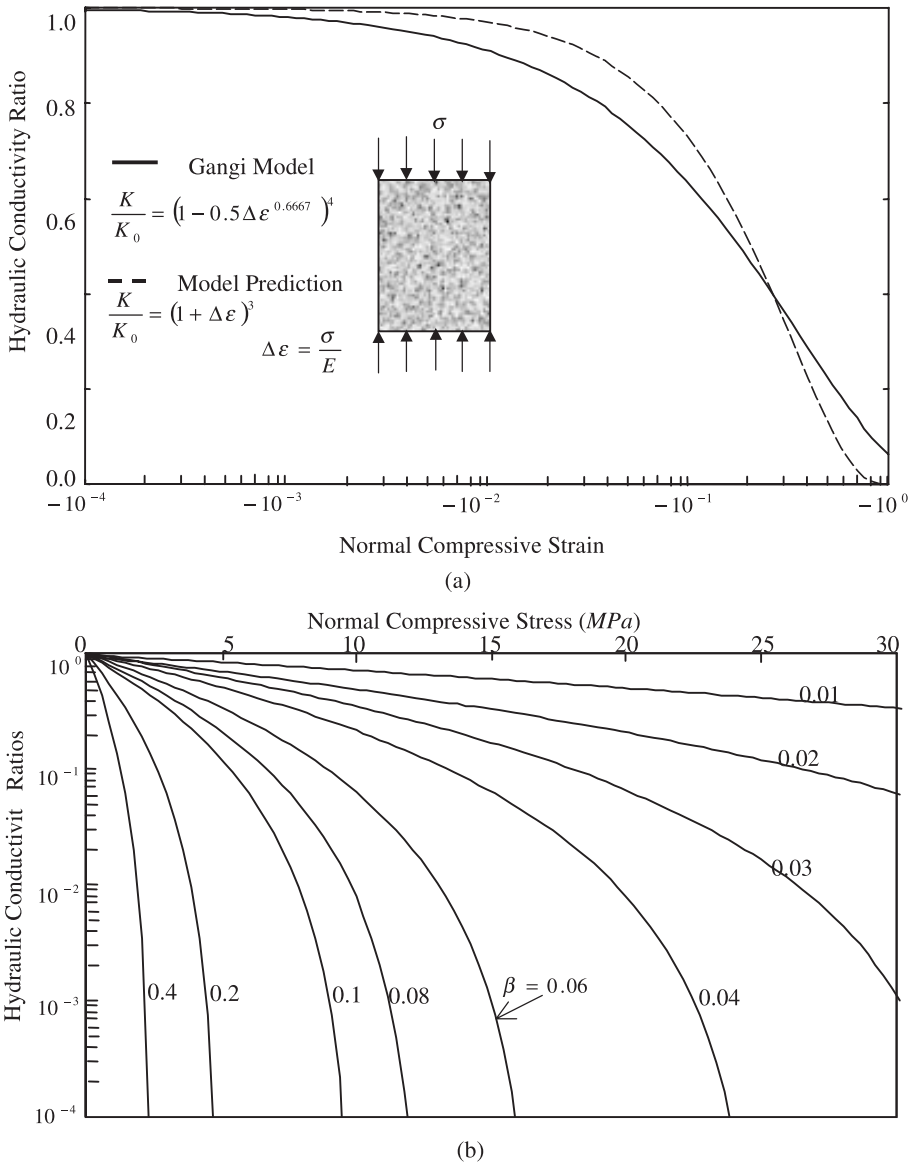

Fig. 3. Analytical results: **a** Comparison with Gangi's model; **b** Relations between normal compressive stress (MPa) and hydraulic conductivity ratios (K/K_0) under different values of β. $\beta = 2(1 - R_e)(1 - \nu)/\phi_f E$ and $\beta = 3(1 - R_e)(1 - 2\nu)/\phi_f E$ for 2-D and 3-D cases, respectively

(conducting) aperture, the following relation for a set of fractures holds

$$K = \frac{ge^3}{12\mu s}, \tag{31}$$

where e is the hydraulic aperture. The empirical relation between mechanical and hydraulic apertures was defined as (Barton et al., 1985)

$$e = \frac{b^2}{\mathrm{JRC}^{2.5}}, \tag{32}$$

where JRC is the fracture roughness and b is the mechanical aperture. Applying Eqs. 31 and 32 for the initial condition, i.e. $e = e_0$, $b = b_0$, and $K = K_0$, yields

$$K_0 = \frac{g e_0^3}{12\mu s} \tag{33}$$

$$e_0 = \frac{b_0^2}{\mathrm{JRC}^{2.5}} \tag{34}$$

respectively. Solving Eqs. 31 through 34 yields

$$K = K_0 \left(\frac{b}{b_0}\right)^6. \tag{35}$$

As apparent from Eq. 35, the conductivity ratios are proportional to the aperture ratio, b/b_0, raised to the power of 6, instead of 3 for the relation proposed in this study. This discrepancy results from the empirical relation between the hydraulic and the mechanical apertures, as apparent in Eq. 32. It is concluded from this comparison that the strain-conductivity relations proposed in this study may need to be modified for closures close to residual apertures, where the influence of fracture roughness is correspondingly more important.

6. Stress-dependent Cubic Flow Laws

For 1-D flow cases, Eq. 2 may be simplified as

$$V = -K(\sigma)\frac{\partial h}{\partial x}, \tag{36}$$

where V is the flow velocity, $K(\Delta\sigma)$ is the stress-dependent hydraulic conductivity, h is the hydraulic head, and x is the spatial coordinate. Flux, Q, may be defined as

$$Q = VA = -K(\Delta\sigma)A\frac{\partial h}{\partial x}, \tag{37}$$

where A is the cross sectional area.

Assuming $\Delta\gamma_{ij} = 0$ $(i, j = x, y, z)$ and $\Delta\varepsilon_{jj} = \Delta\varepsilon_{kk}$, Eqs. 15 and 16 may be symbolically rewritten as

$$\frac{K_{ii}}{K_0} = (1 + \beta\Delta\sigma_{jj})^3, \tag{38}$$

where β is defined, for 2-D and 3-D cases, as

$$\beta = \frac{2(1 - R_e)(1 - v)}{\phi_f E} \tag{39}$$

$$\beta = \frac{3(1 - R_e)(1 - 2v)}{\phi_f E}, \tag{40}$$

respectively. The relations between normal compressive stress and hydraulic conductivity ratio are illustrated for different values of β in Fig. 3(b). It is apparent that the normal compressive stress may have significant impact on the hydraulic conductivity and the impact is regulated by the value of β.

Substituting Eqs. 38 into 37 yields

$$Q = -AK_0(1 + \beta\Delta\sigma)^3 \frac{\partial h}{\partial x} \tag{41}$$

where β is defined by Eqs. 39 or 40. Equation 41 may be defined as a stress-dependent cubic law. The equation is rewritten as

$$\frac{Q}{Q_0} = (1 + \beta\Delta\sigma)^3; \tag{42}$$

where Q_0 is the flux under the condition of a null stress change, $\Delta\sigma = 0$. The most obvious advantage in applying this cubic law is that no additional elusive material parameters are introduced, and that all parameters are commonly available in practice. This advantage makes it possible to verify the proposed model against experimental data. Verifications against Skoczylas and Henry's experimental data (1995) and Myer's data (1991) are shown in Fig. 4. The analytical results agree well with the experimental data. It should be pointed out that the values of β, used in these verifications, are assumed as insufficient data are available.

7. Conclusions

The hydraulic response of a fractured medium to applied deformations has been evaluated by the development of constitutive relations linking applied strains to resulting changes in hydraulic conductivities. The obvious advantage of these relations is that the parameters they require are available in practice. More importantly, the incorporation of RQD and RMR enables the stress-dependent hydraulic conductivity to represent a broad spectrum of rock masses varying from highly fractured (crushed) rock to intact rock. These two empirical parameters determine the hydraulic response of a fractured medium to induced-deformations. Analytical results indicate that directional hydraulic conductivities in porous media are relatively insensitive to changes in strain because of the close spacing of the flow conduits, relative to the conduit apertures. However, both normal and shear strains exercise significant control on the directional hydraulic conductivity ratios of fractured media. The magnitudes of these ratios are primarily modulated by two rock mass classification indexes, RMR and RQD. Depending on the magnitudes of these two empirical parameters, these ratios may increase or decrease by several orders of magnitude. Extensional strains increase the directional conduc-

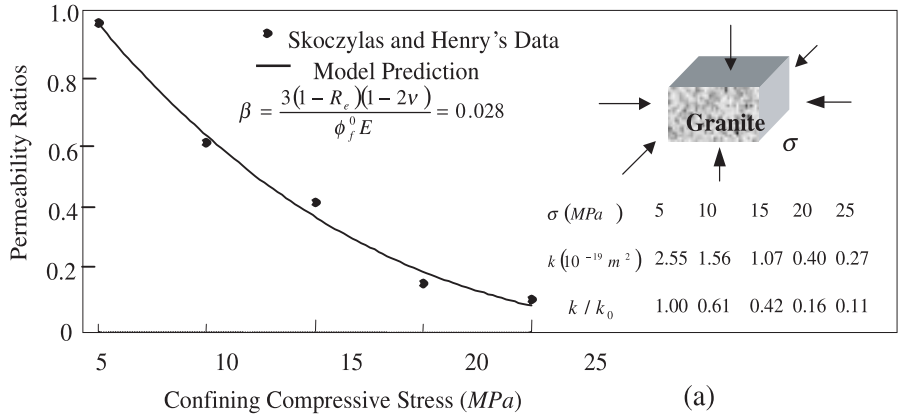

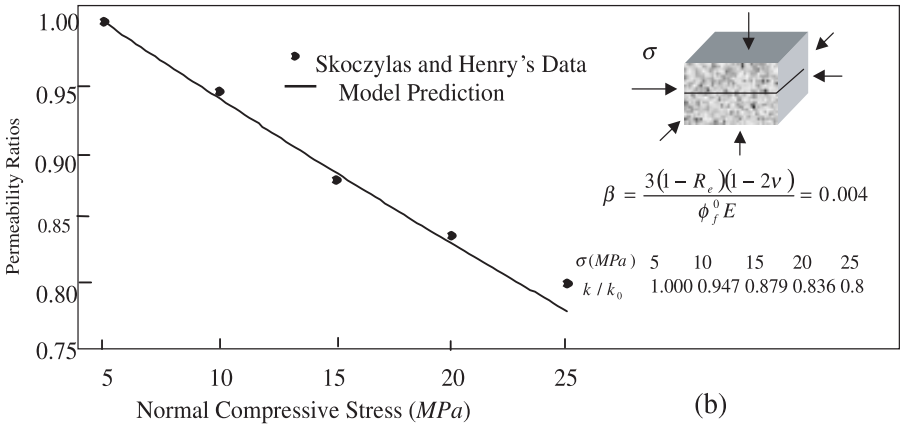

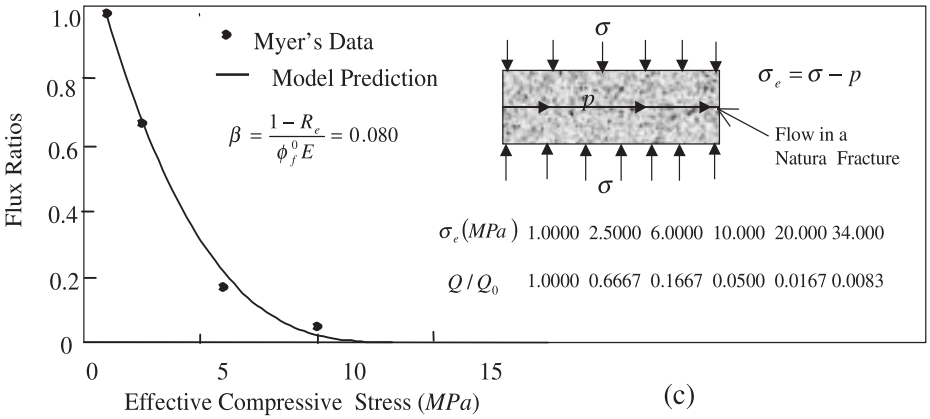

Fig. 4. Comparison of the model predictions with Skoczylas and Henry's experimental data for porous rock **(a)** and for fractured rock **(b)**, and with Myer's experimental data of flow in a natural fracture **(c)**

tivity by incrementing the aperture, compressive strains decrease the conductivity due to the reduction in aperture. Under low ambient stress levels, shear strains always result in increased hydraulic conductivity due to the dilatancy of fractures.

These constitutive relations, linking applied strains and hydraulic conductivities, may be applied in a variety of engineering fields where mining, petroleum or geothermal energy production, degasification or *in-situ* mining, among other processes, induce strains within geologic media. Despite this widespread applicability, caution should be exercised in their application, ensuring that their limitations are not violated. Principal limitations relate to the presumed validity of the cubic law for flow in a single fracture and the elastic response of both rock matrix and the rock mass deformation.

Acknowledgments

The work reported in this paper was supported by Schlumberger International through the Stiching Foundation Award and by the National Science Foundation under Grant No. MSS-9209059. The sources of this support are gratefully acknowledged. The authors also thank two anonymous reviewers for providing critical comments and constructive suggestions in revising the manuscript.

References

Alvarez T. A., Cording, E. J., Mikhail, R. E. (1995): Hydromechanical behavior of rock joints: A re-interpretation of published experiments. In: Daemen, J. J. K., Schiltz, R. A. (eds.) Proc., 35th U. S. Symposium on Rock Mechanics, 665–671.

Ayatollahi, M. S., Noorishad, J., Witherspoon, P. A. (1983): Stress-fluid flow analysis of fractured rock. J. Eng. Mech. 109, 1–13.

Barton, N., Bandis, S., Bakhtar, K. (1985): Strength, deformation and conductivity coupling of rock joints. Int. J. Rock Mech. Min. Sci. Geomech. Abstr. 22, 121–140.

Bawden, W. F., Curran, H., Roegiers, J. C. (1980): Influence of fracture deformation on secondary permeability-a numerical approach. J. Int. Rock Mech. Min. Sci. Geomech. Abstr. 17, 265–279.

Bieniawski, Z. T. (1978): Determinating rock mass deformability: experience from case histories. Int. J. Rock Mech. Min. Sci. Geomech. Abstr. 15(3), 237–248.

Booth, C. J. (1992): Hydrogeologic impacts of underground (longwall) mining in the Illinois basin. In: Peng S. S., (ed.) Proc., Third Workshop on Surface Subsidence due to Underground Mining, Department of Mining Engineering, West Virginia University, Morgantown, 222–227.

Brown, S. R. (1987): Fluid flow through rock joints: the effect of surface roughness. J. Geophys. Res. 92, 1337–1347.

Gangi, A. F. (1978): Variation of whole and fractured porous rock permeability with confining pressure. Int. J. Rock. Mech. Min. Sci. Geomech. Abstr. 15(3), 249–257.

Hooper, E. C. D. (1990): Fluid migration along growth faults in compacting sediments. J. Pet. Geol. 14, 161–180.

Jakubick, A. T., Franz, T. (1993): Vacuum testing of the permeability of the excavation damage zone. Rock Mech. Rock Engng. 26(2), 165–182.

Jones, F. O. (1975): A laboratory study of the effects of confining pressure on fracture flow and storage capacity in carbonate rocks. J. Pet. Tech. 27, 21–27.

King, M. S., Chaudhry, N. A., Shakeel, A. (1995): Experimental ultrasonic velocities and permeability for sandstones with aligned cracks. Int. J. Rock Mech. Geomech. Abstr. 32(2), 155–163.

Kranz, R. L. (1979): The permeability of whole and jointed barre granite. Int. J. Rock Mech. Min. Sci. Geomech. Abstr. 16, 225–234.

Li, et al. (1994): Permeability-strain equations corresponding to the complete stress-strain path of Yinzhuang sandstone. Int. J. Rock Mech. Min. Sci. Geomech. Abstr. 31(4), 383–391.

Liu, J. (1994): Topographic influence of longwall mining on water supplies. Master's thesis, Department of Mineral Engineering, The Pennsylvania State University, University Park.

Liu, J. (1996): Numerical studies toward a determination of the impact of longwall mining on groundwater resources. PhD thesis, The Pennsylvania State University, University Park.

Liu, J., Elsworth, D. (1997): Three-dimensional effects of hydraulic conductivity enhancement and desaturation around mined panels. Int. J. Rock Mech. Min. Sci. Geomech. Abstr. 34(8), 1139–1152.

Liu, J., Elsworth, D., Matetic, R. J. (1997): Evaluation of the post-mining groundwater regime following longwall mining. Hydrol. Processes 11, 1945–1961.

Makurat, A. N. (1985): The effect of shear displacement on the permeability of natural rough joints. In: Newman, S. P. (ed.) Hydrogeology of rocks of low permeability, vol. 17, 99–106.

Makurat, A., Gutierrez, M. (1996): Constitutive modeling of faulted/fractured reservoirs. In: Proc., Hydrocarbon Seals-Importance for Exploration and Production.

Makurat, A., Barton, N., Rad, N. S. (1990): Joint conductivity variation due to normal and shear deformation. In: Barton, N., Stephansson, O. (eds.) Rock joints. 535–540.

Matetic, R. J. (1993): An assessment of longwall mining-induced changes in the local groundwater system. In: Proc., FOCUS Conference on Eastern Regional Ground Water Issues, 27–29.

Matetic, R. J., Trevits, M. (1992): Longwall mining and its effects on ground water quantity and quality at a mine site in the Northern Applachian coal field. In: Proc., FOCUS Conference on Eastern Regional Ground Water Issues, 13–15.

Matetic, R. J., Trevits, M. A., Swinehart, T. (1991): A case study of longwall mining and near-surface hydrological response. In: Proc., American Mining Congress-Coal Convention, Pittsburgh, PA.

Matetic, R. J., Liu, J., Elsworth, D. (1995): Modeling the effects of longwall mining on the groundwater system. In: Daemen, J. J. K., Schiltz, R. A. (eds.) Proc., 35th U. S. Symposium on Rock Mechanics, 639–644.

Mohammad, N., Reddish, D. J., Stace, L. R. (1997): The relation between in-situ and laboratory rock properties used in numerical modeling. Int. J. Rock Mech. Min. Sci. Geomech. Abstr. 34(2), 289–297.

Myer, L. D. (1991): Hydromechanical and seismic properties of fractures. In: Proc., 7th International Rock Mechanics Congress, vol. 1, 397–409.

Neate, C. J., Whittaker, B. J. (1979): Influence of proximity of longwall mining on strata

permeability and ground water. In: Proc., U.S. 22nd Symposium on Rock Mechanics, The University of Texas, Austin, 217–224.

Nelson, R. A., Handin, J. (1977): Experimental study of fracture permeability in porous rock. Am. Assoc. Petrol. Geol. Bull. 61, 227–236.

Nicholson, G. A., Bieniawski, Z. T. (1990): A nonlinear deformation modulus based on rock mass classification. Int. J. Min. Geol. Engng. 8, 181–202.

Ouyang, Z., Elsworth, D. (1993): Evaluation of groundwater flow into mined panels. Int. J. Rock Mech. Min. Sci. Geomech. Abstr. 30(2), 71–79.

Patton, S. B., Fan, H., Novak, T., Johnson, P. W., Sanford, R. L. (1994): Simulator for degasification, methane emission prediction and mine ventilation. Min. Engng. (April), 341–345.

Priest, S. D., Hudson, J. (1976): Discontinuity spacing in rock. Int. J. Rock Mech. Min. Sci. Geomech. Abstr. 13, 135–148.

Pusch, R. (1989): Alteration of the hydraulic conductivity of rock by tunnel excavation. Int. J. Rock Mech. Min. Sci. Geomech. Abstr. 26(1), 79–83.

Roosendaal, D. J. Van et al. (1990): Overburden deformation and hydrological changes due to longwall mine subsidence in Illinois. In: Chugh, Y. P. (ed.) Proc., 3rd Conference on Ground Control Problems in the Illinois Coal Basin, Mt. Vernon, IL, 73–82.

Sen, Z. (1997): Theoretical RQD-porosity-conductivity-aperture charts. Int. J. Rock Mech. Min. Sci. Geomech. Abstr. 33(2), 173–177.

Skoczylas, F., Henry, J. P. (1995): A study of the intrinsic permeability of granite to gas. Int. J. Rock Mech. Min. Sci. Geomech. Abstr. 32(2), 171–179.

Smelser, R. E., Richmond, O., Schwerer, F. C. (1984): Interaction of compaction near mine openings and drainage of pore fluids from coal seams. Int. J. Rock Mech. Min. Sci. Geomech. Abstr. 21, 13–20.

Teufel, L. W. (1987): Permeability changes during shear deformation of fractured rock. In: Proc., 28th U.S. Symposium on Rock Mechanics, 473–480.

Trimmer, D., Bonner, D., Heard, C. H., Duba, A. (1980): Effect of pressure and stress on water transport in intact and fractured gabbro and granite. J. Geophys. Res. 85, 7059–7071.

Valliappan, S., Zhang, W. (1996): Numerical modeling of methane gas migration in dry coal seams. Int. J. Numer. Analyt. Meth. Geomech. 20, 571–593.

Walker, J. S. (1988): Case study of the effects of longwall mining induced subsidence on shallow groundwater sources in the Northern Appalachian Coalfield. RI9198, Bureau of Mines, US Department of the Interior.

Wei, Z. Q., Egger, P., Descoeudres, F. (1995): Permeability predictions for jointed rock masses. Int. J. Rock Mech. Min. Sci. Geomech. Abstr. 32(3), 251–261.

Witherspoon, P. A., Wang, J. S. Y., Iwai, K., Gale, J. E. (1980): Validity of cubic law for fluid flowin a deformable rock fracture. Water Resour. Res. 16(6), 1016–1024.

Zhang, L., Franklin, J. A. (1993): Prediction of water flow into rock tunnels: an analytical solution assuming an hydraulic conductivity gradient. Int. J. Rock Mech. Min. Sci. Geomech. Abstr. 30(1), 37–46.

Authors' address: Jishan Liu, CSIRO Exploration and Mining, Environmental Engineering Group, Private Bag, PO Wembley, WA6014, Australia.